Supplementary Information for -

An epithelial *Nfkb2* pathway exacerbates intestinal inflammation by supplementing latent RelA dimers to the canonical NF-κB module

Meenakshi Chawla[1], Tapas Mukherjee[1,2], Alvina Deka[1], Budhaditya Chatterjee[1,3], Uday Aditya Sarkar[1], Amit K. Singh[4], Saurabh Kedia[4], Josephine Lum[5], Manprit Kaur Dhillon[5], Balaji Banoth[1,6], Subhra K. Biswas[5], Vineet Ahuja[4], Soumen Basak[1,*]

[1]Systems Immunology Laboratory, National Institute of Immunology, Aruna Asaf Ali Marg, New Delhi-110067, India
[2]Current Address: Department of Immunology, University of Toronto, Canada
[3]Indian Institute of Technology Delhi, New Delhi-110016, India
[4]All India Institute of Medical Science, New Delhi-110023, India
[5]Singapore Immunology Network, Agency for Science, Technology and Research (A*STAR)
[6]Current Address: Department of Immunology, St. Jude Children's Research Hospital, USA

Correspondence should be addressed to S.B.

Figure S1 – Figure S5;

Supplementary Table S1-S4;

Supplementary Methods

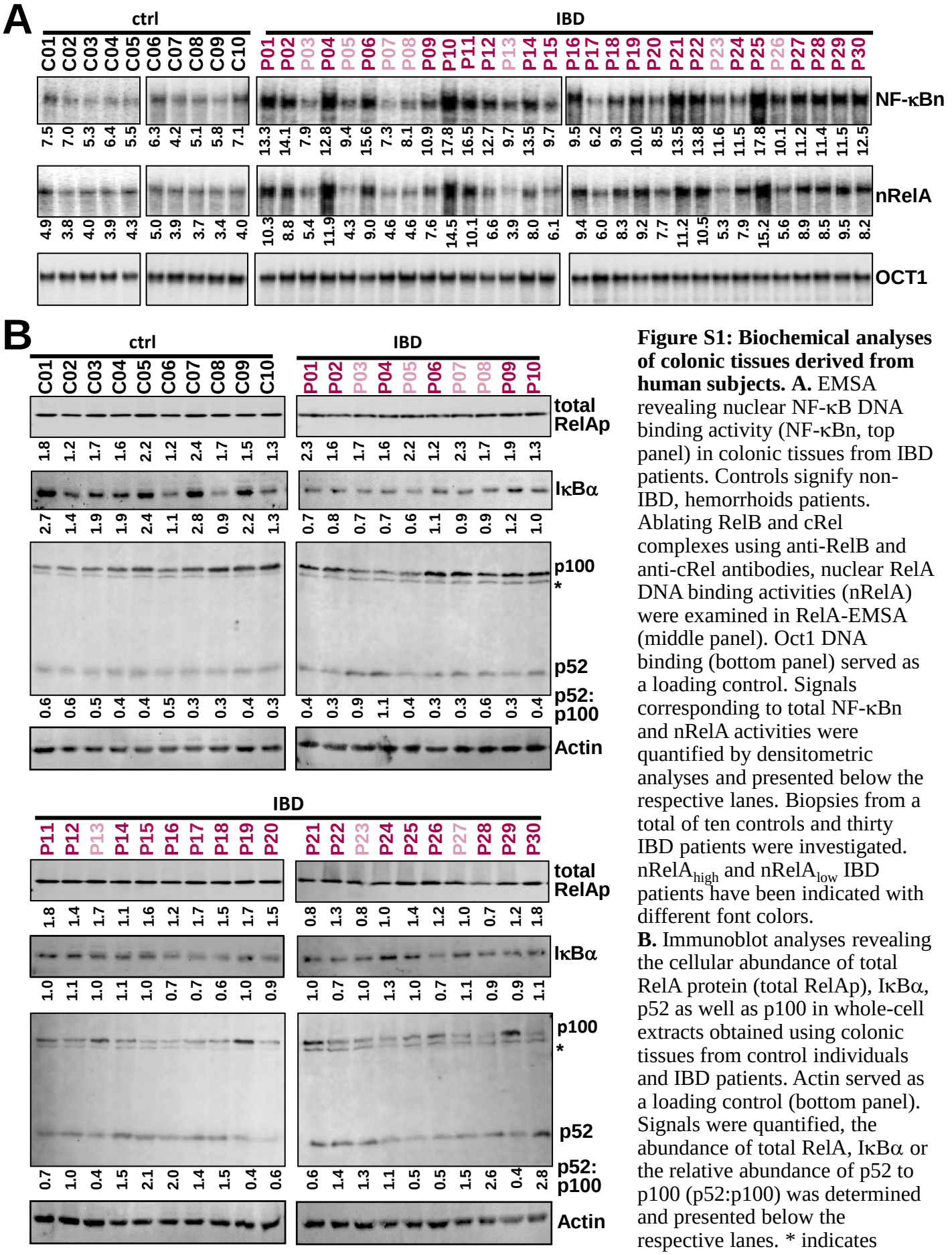

Figure S1: Biochemical analyses of colonic tissues derived from human subjects. A. EMSA revealing nuclear NF-κB DNA binding activity (NF-κBn, top panel) in colonic tissues from IBD patients. Controls signify non-IBD, hemorrhoids patients. Ablating RelB and cRel complexes using anti-RelB and anti-cRel antibodies, nuclear RelA DNA binding activities (nRelA) were examined in RelA-EMSA (middle panel). Oct1 DNA binding (bottom panel) served as a loading control. Signals corresponding to total NF-κBn and nRelA activities were quantified by densitometric analyses and presented below the respective lanes. Biopsies from a total of ten controls and thirty IBD patients were investigated. $nRelA_{high}$ and $nRelA_{low}$ IBD patients have been indicated with different font colors.

B. Immunoblot analyses revealing the cellular abundance of total RelA protein (total RelAp), IκBα, p52 as well as p100 in whole-cell extracts obtained using colonic tissues from control individuals and IBD patients. Actin served as a loading control (bottom panel). Signals were quantified, the abundance of total RelA, IκBα or the relative abundance of p52 to p100 (p52:p100) was determined and presented below the respective lanes. * indicates

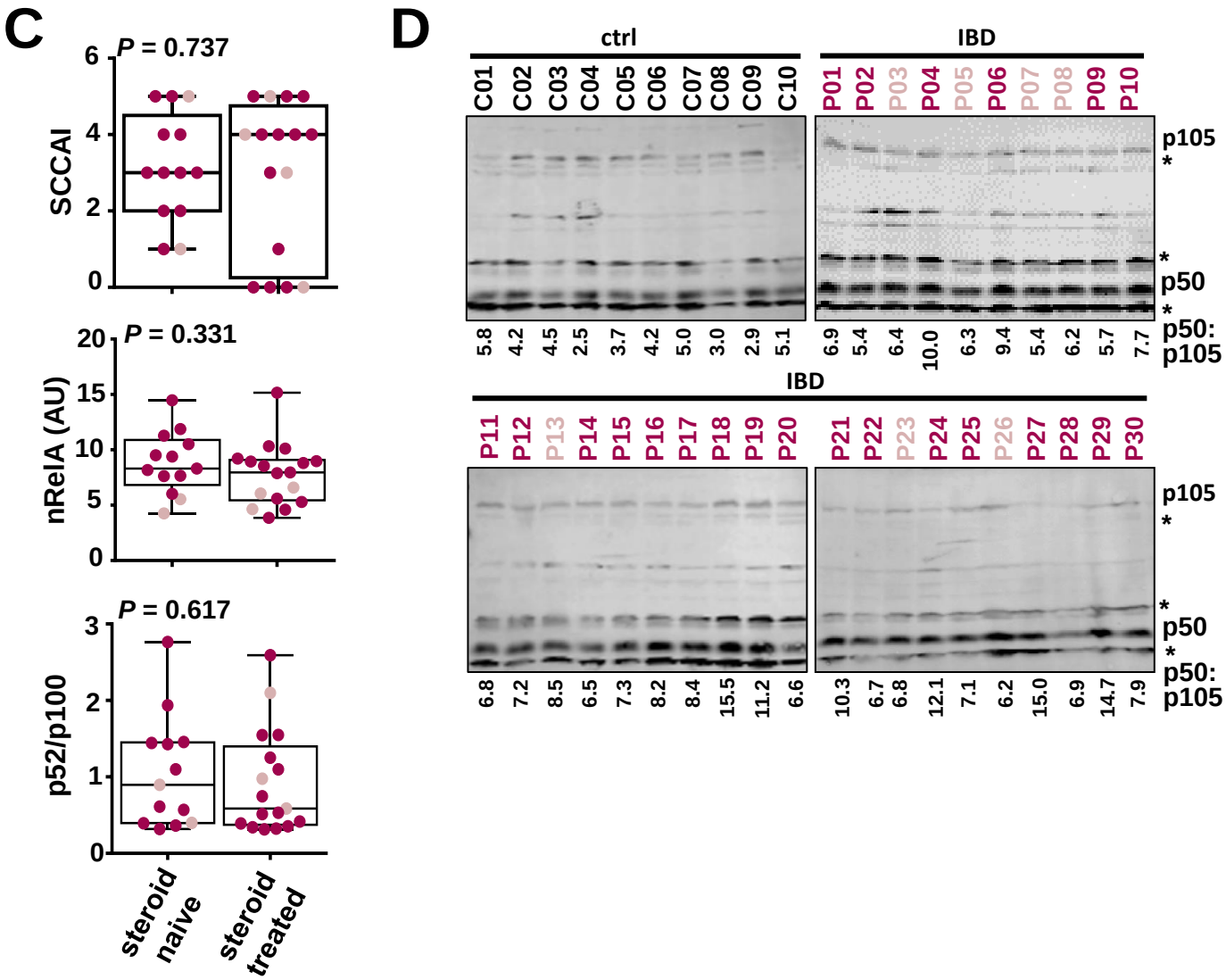

[Fig S1 continued] nonspecific protein bands ascertained using WT or *Nfkb2*$^{-/-}$ cell extracts. **C.** Comparing steroid-naïve and steroid-treated patients for disease severity, nRelA activity and p100 processing. The cohort consisted of thirteen steroid-naïve and seventeen steroid-treated patients. Disease activity in UC was measured by Simple Clinical Colitis Activity Index (SCCAI). Disease activity status of one individual was unknown. **D.** Immunoblot analyses was performed for detecting p50 and p105 in whole-cell extracts from controls and IBD patients. Signals were quantified and the relative abundance of p50 to p105 (p50:p105) was determined and presented below the respective lanes. * indicates nonspecific protein bands ascertained using WT or *Nfkb1*$^{-/-}$ cell extracts.

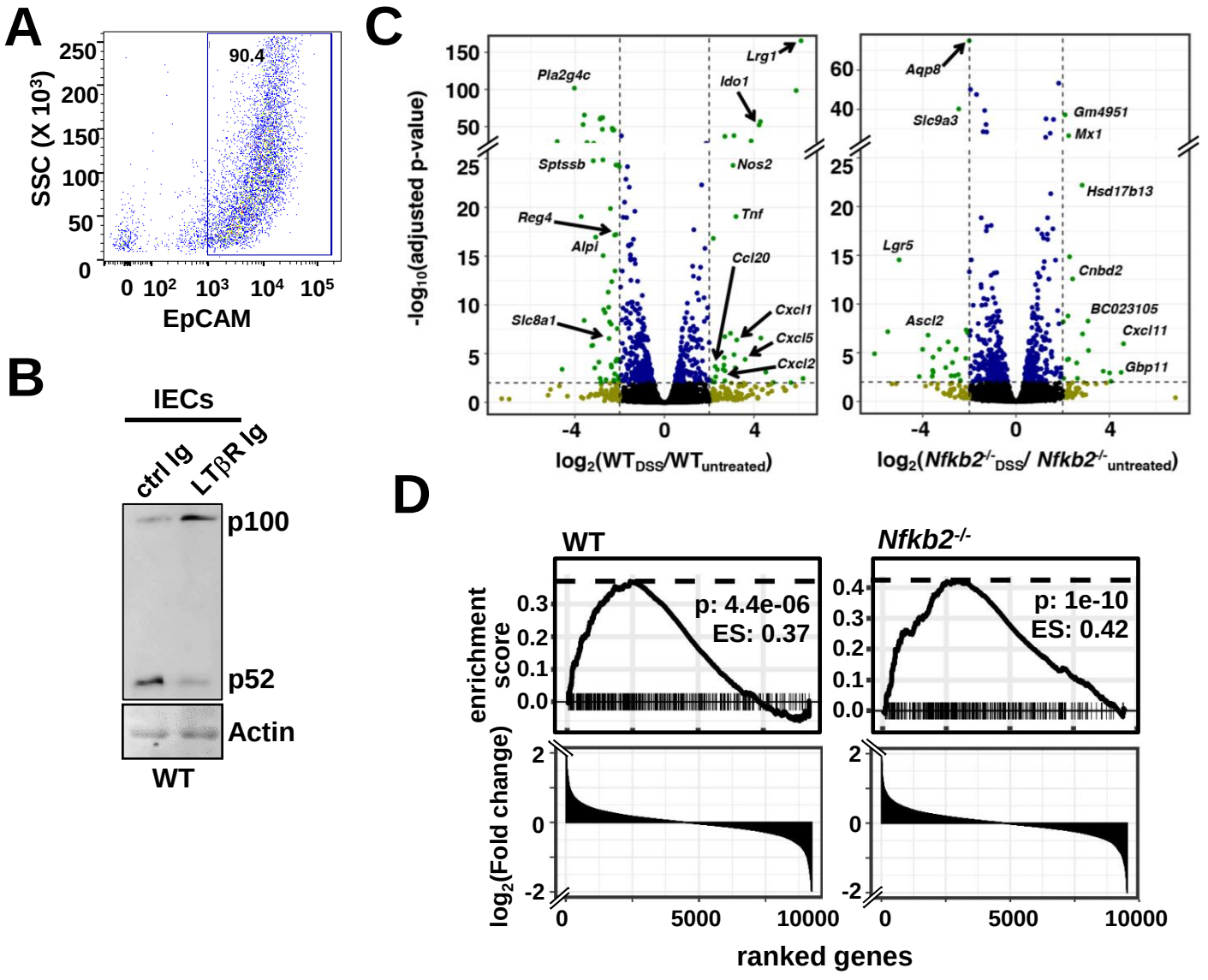

Figure S2: Investigating the *Nfkb2* pathway in IECs from colitogenic mice. A. FACS plots revealing enrichment of EpCAM+ cells in our mouse IEC preparation. **B.** Immunoblot of whole-cell extracts derived from IECs from WT mice administered with control-Ig or LTβR-Ig 24h prior to tissue collection. **C.** Volcano plots depicting the fold change in the mRNA level in IECs upon 48h of 2.5% DSS treatment of WT or *Nfkb2*$^{-/-}$ mice. The global gene expression data represents three biological replicates subjected to RNA-seq analyses. The horizontal dashed line represents p-value = 0.01. The green dots represent genes, whose expressions were at least four fold different in a stastistically significant manner. **D.** GSEA revealing enrichment of the goblet cell-specific gene signature among genes induced in IECs upon DSS treatment of WT or global *Nfkb2*$^{-/-}$ mice. Excluding transcripts in the RNA-seq data with the cumulative read count encompassing all six sets for a given genotype below 250, we focused on a list of 9271 and 9546 genes for WT and *Nfkb2*$^{-/-}$ mice, respectively. Data represent means ± SEM. Statistical significance was determined bytwo-tailed Student's t-test. ** P<0.01.

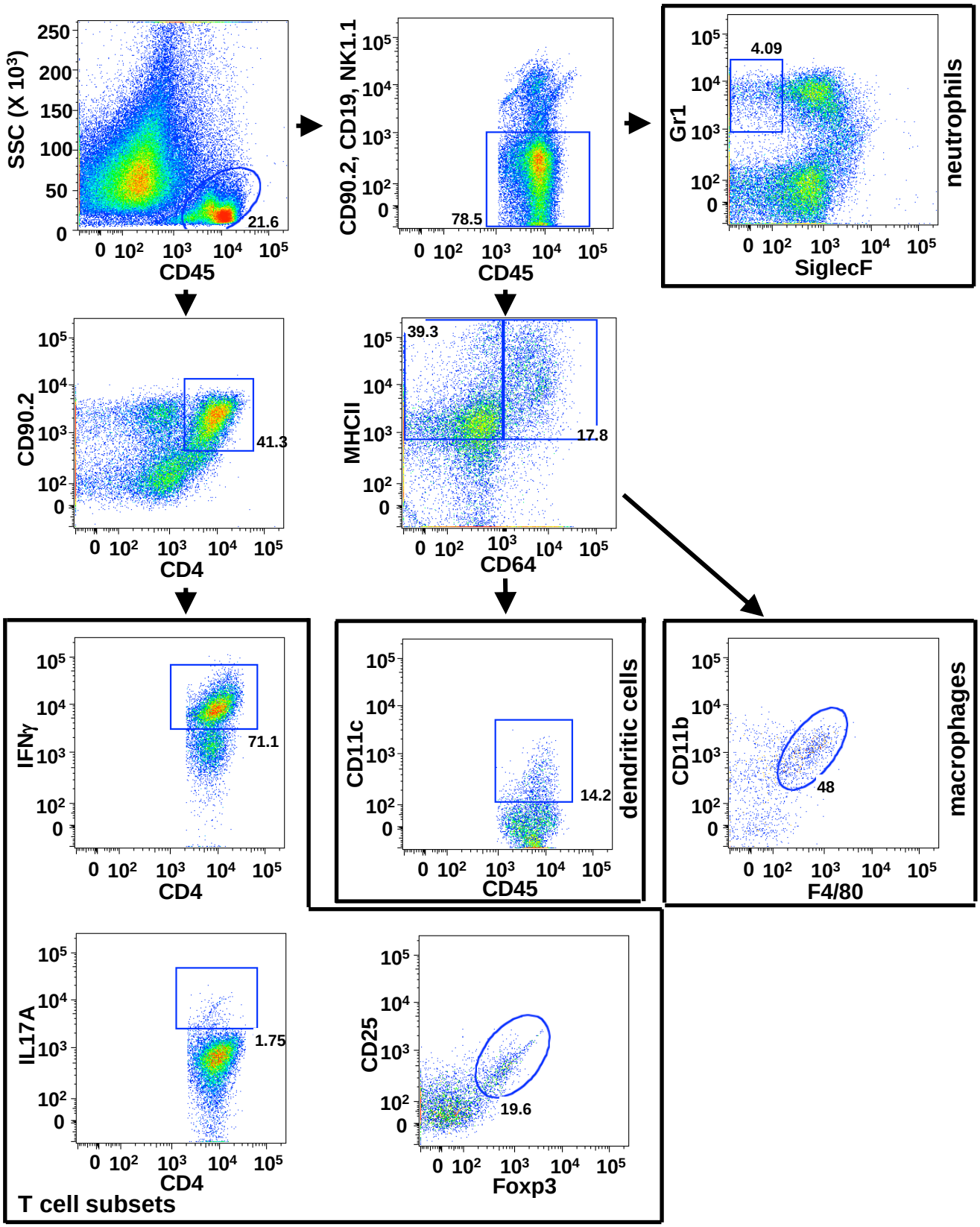

Figure S3: Investigating immune cells in the colitogenic gut of WT and *Nfkb2*$^{-/-}$ mice. Representative FACS plots showing the general gating strategy for analysing the frequencies of neutrophils, macrophages, dendritic cells, and variout T cell subsets in the lamina propria. The data represent WT mice treated with DSS for five days. Similarly, frequencies of these cells were also measured in DSS-treated *Nfkb2*$^{-/-}$ mice.

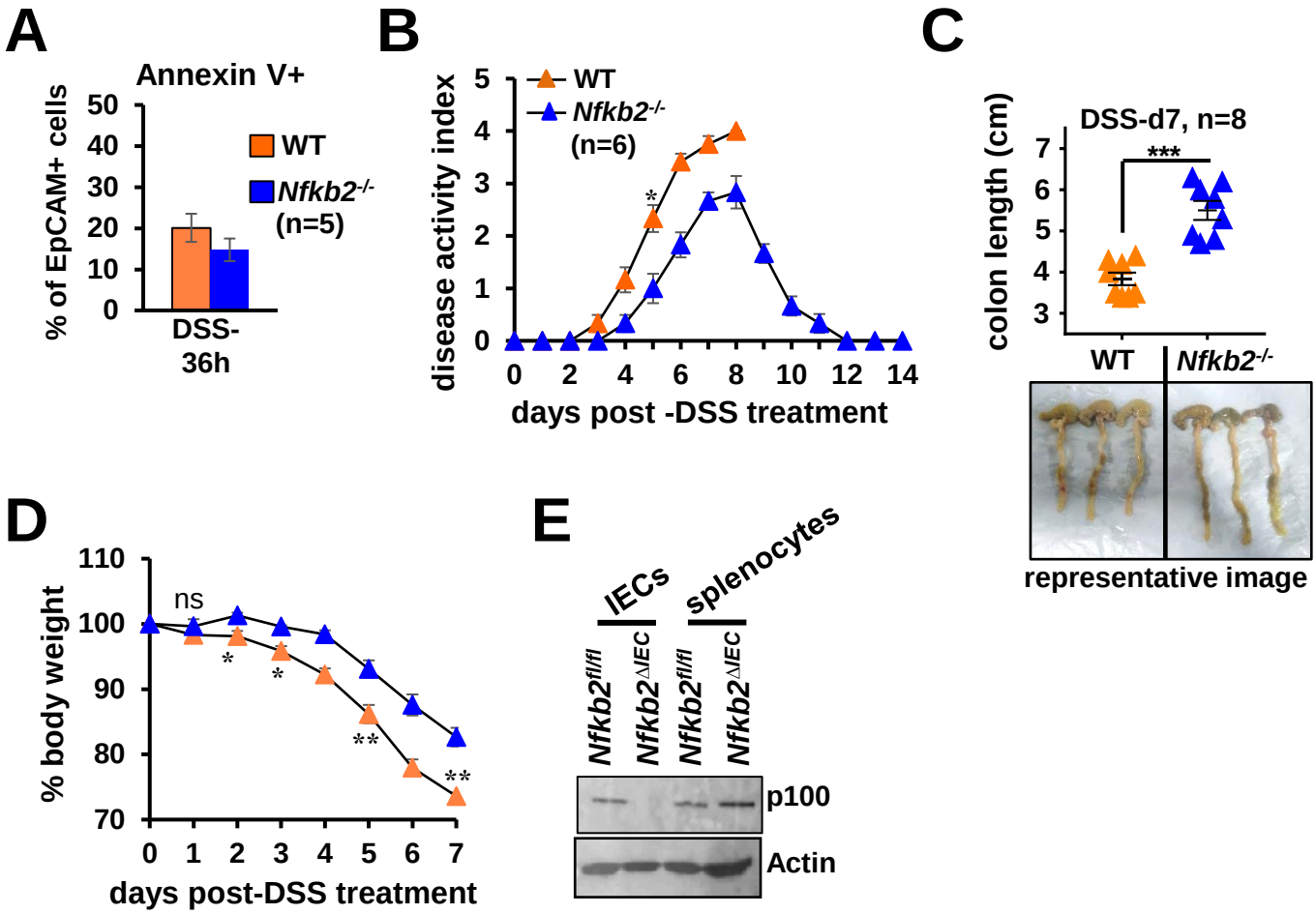

Figure S4: Comparing WT and *Nfkb2*$^{-/-}$ mice for colitogenic phenotypes. A. WT and *Nfkb2*$^{-/-}$ mice were administered with 2.5% DSS for 36h, subequently IECs were collected and examined for the presence of Annexin V+ apoptotic cells; the data has been corrected for corresponding basal apoptosis observed in untrated mice. **B to D.** Alternatly, mice were treated with DSS for seven days and evaluated for the disease activity **(B)**, colon length **(C)** and and bodyweight changes **(D)**. In the case of WT, disease activity measurements were discontinued after nine days because of morbidity and mortality **(B)**. Colon length was measured at day seven from the onset of DSS treatment; representative images of colons derived from DSS-treated WT or *Nfkb2*$^{-/-}$ mice have also been shown **(C)**. Bodyweight changes were scored in a time course **(D)**. **E.** Representative immunoblot revealing the abundance of p100/*Nfkb2* in IECs and spleenocytes derived from *Nfkb2*$^{fl/fl}$ and *Nfkb2*$^{\Delta IEC}$ mice. Statistical significance was determined by two-tailed Student's t-test. ***$P < 0.001$; **$P < 0.01$; *$P < 0.05$.

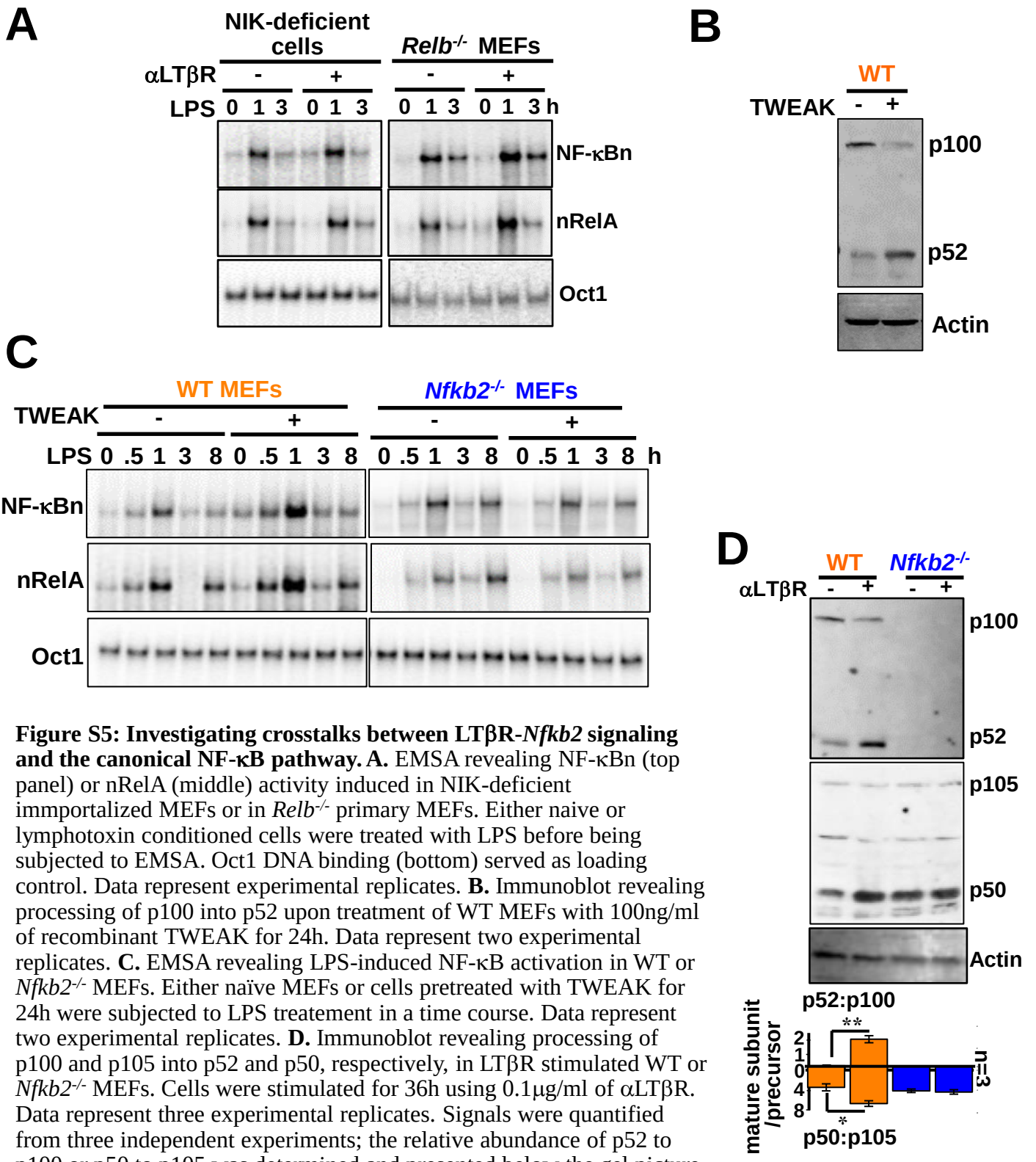

Figure S5: Investigating crosstalks between LTβR-*Nfkb2* signaling and the canonical NF-κB pathway. A. EMSA revealing NF-κBn (top panel) or nRelA (middle) activity induced in NIK-deficient immportalized MEFs or in *Relb*$^{-/-}$ primary MEFs. Either naive or lymphotoxin conditioned cells were treated with LPS before being subjected to EMSA. Oct1 DNA binding (bottom) served as loading control. Data represent experimental replicates. **B.** Immunoblot revealing processing of p100 into p52 upon treatment of WT MEFs with 100ng/ml of recombinant TWEAK for 24h. Data represent two experimental replicates. **C.** EMSA revealing LPS-induced NF-κB activation in WT or *Nfkb2*$^{-/-}$ MEFs. Either naïve MEFs or cells pretreated with TWEAK for 24h were subjected to LPS treatement in a time course. Data represent two experimental replicates. **D.** Immunoblot revealing processing of p100 and p105 into p52 and p50, respectively, in LTβR stimulated WT or *Nfkb2*$^{-/-}$ MEFs. Cells were stimulated for 36h using 0.1μg/ml of αLTβR. Data represent three experimental replicates. Signals were quantified from three independent experiments; the relative abundance of p52 to p100 or p50 to p105 was determined and presented below the gel picture.

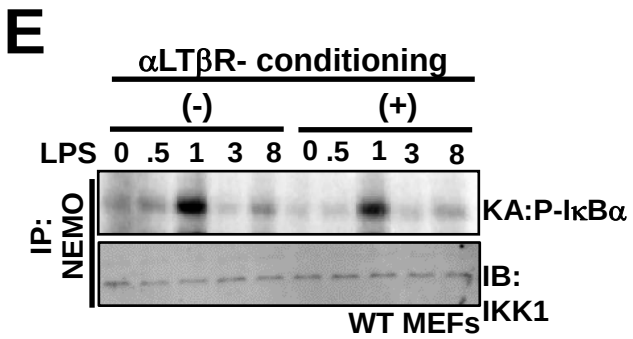

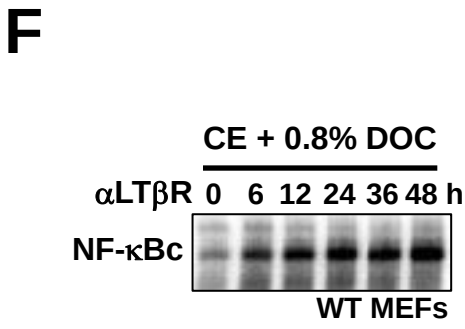

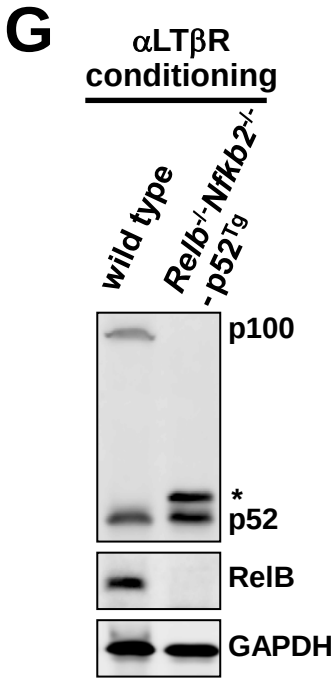

[Fig S5 continued] E. Kinase assay revealing the activation of the NEMO-IKK2 complex in MEFs upon LPS treatment. Cells were either left untreated or treated with 0.1μg/ml of αLTβR agonistic antibody, which activates the noncanonical pathway, for 36h before being subjected to LPS stimulation. Subsequently, NEMO co-immunoprecpipitates obtained from these cells were incubated with recombinant GST-IκBα for scoring the NEMO-IKK2 activity. IKK1 co-immunoprecipitated with NEMO was probed as loading control. Data represent two experimental replicates. **F.** EMSA revealing gradual accumulation of latent NF-κB complexes in the cytoplasm of cells subjected to αLTβR stimulation (0.1μg/ml of αLTβR). Cytoplasmic extracts were treated with deoxycholate before being subjected to EMSA for unmasking latent NF-κB DNA binding activities. **G.** Immunoblot revealing p52 expressions from a retroviral transgene in immortalized *Relb*$^{-/-}$*Nfkb2*$^{-/-}$ MEFs subjected to lymphotoxin-conditioning.

Supplementary Table S1: antibodies used

Reagent	Source	Identifier
Antibodies		
RelA Rabbit Polyclonal IgG	Santa Cruz Biotechnology	sc-372
RelB Rabbit Polyclonal IgG	Santa Cruz Biotechnology	sc-226
cRel Rabbit Polyclonal IgG	Santa Cruz Biotechnology	sc-71
IκBα Rabbit Polyclonal IgG	Santa Cruz Biotechnology	sc-371
Nfkb2 p100/p52 Antibody	Cell Signaling Technology	4882
Anti-p50 Antibody	BioBharati LifeSciences	BB-AB0080
Anti-NEMO Antibody	BioBharati LifeSciences	BB-AB0035
IKK1 Rabbit Polyclonal IgG	Santa Cruz Biotechnology	sc-7184
β-Actin Goat Polyclonal IgG	Santa Cruz Biotechnology	sc-1615
Goat anti-Rabbit IgG-HRP Secondary Antibody	Santa Cruz Biotechnology	sc-2004
Donkey anti-Goat IgG-HRP Secondary Antibody	Santa Cruz Biotechnology	sc-2020
Goat anti-Rabbit IgG-Cy5 Secondary Antibody	GE-Healthcare	29038278
Rabbit Trueblot Anti-Rabbit IgG HRP	Rockland	18-8816-33
Anti-mouse CD45.2 APC Antibody	eBiosciences	17-0454-82
Anti-mouse CD45.1 PE Antibody	eBiosciences	12-0453-82
Anti-mouse EpCAM PE Antibody	eBiosciences	12-5791-82
Anti-mouse CD90.2 FITC Antibody	Biolegend	105306
Anti-human/mouse CD45R PE Antibody	eBiosciences	12-0452-82
Anti-mouse CD19 FITC Antibody	eBiosciences	11-0191-82
Anti-mouse NK1.1 FITC Antibody	eBiosciences	11-5941-82
Anti-mouse CD11b brilliant violent 510 Antibody	Biolegend	101245
Anti-mouse CD11c PerCP Antibody	Biolegend	117236

continued

Supplementary Table S1: antibodies used

Reagent	Source	Identifier
Antibodies		
Anti-mouse Lys-6G FITC Antibody	eBiosciences	11-9668-82
Anti-mouse F4/80 eFluor 450 Antibody	eBiosciences	48-0251-82
Anti-mouse MHCII PE-Cy7 Antibody	eBiosciences	25-5321-82
Anti-mouse CD64 PerCP-e710 Antibody	eBiosciences	46-0641-82
Anti-mouse CD4 PE-Cy7 Antibody	eBiosciences	25-0041-82
Anti-mouse CD25 eFluor 450 Antibody	eBiosciences	48-0251-82
Anti-mouse IFNg APC-Cy7 Antibody	Biolegend	505850
Anti-mouse/rat IL17A PerCP-Cy5.5 Antibody	eBiosciences	45-7177-82
Anti-mouse/rat Foxp3 FITC Antibody	eBiosciences	11-5773-82
Anti-mouse Siglec F APC-Cy7 Antibody	BD Bioscience	565527
Chemicals and Peptides		
DSS (36,000-50,000 MW)	MP Biomedicals	160110
FITC-Dextran (MW 3000 - 5000)	Sigma-Aldrich	60842-46-8
Agonistic LTbR antibody (aLTbR), AFH6	Biogen Inc., USA	AFH6
Antagonistic LTβR-Ig Antibody	Biogen Inc., USA	N/A
Control MOPC21 Antibody	Biogen Inc., USA	N/A
Recombinant mouse TWEAK	R&D Systems	1237-TW-025
Collagenase, Type 4	Worthington	LS004188
DNase I	Worthington	LS002139
LPS from E.coli serotype O55:B5	Enzo Life Sciences	ALX-581-013-L002
Recombinant GST-IkBa (1-54) protein	BioBharati Life Sciences	Customized

Supplementary Table S2: Key commercial kits

Commercial Kits		
RNeasy Mini Kit (250)	Qiagen	74106
Primescript 1st strand cDNA synthesis kit	Takara Bio	6110B
Foxp3/Transcription Factor Staining Buffer Set	eBioscience	00-5523-00

Supplementary Table S3: animal strains

Mice models		
C57BL/6 WT mice	available at the Small Animal Facility in NII	N/A
C57BL/6 SJL mice	Jackson Laboratories	002014
Nfkb2$^{-/-}$ mice	available at the Small Animal Facility in NII.	N/A
Nfkb2$^{fl/fl}$ mice	Jackson Laboratories	028720
Villin-Cre mice	gift from Prof. Florian Greten, Georgspeyer-Haus Institute of Tumor Biology and Experimental Therapy, Germany.	N/A
Nfkb2$^{\Delta IEC}$ mice	generated by crossbreeding *Nfkb2*$^{fl/fl}$ mice with Villin-Cre mice.	N/A

Supplementary Table S4: primers for RT-qPCR

Gene	**Forward Primer**	**Reverse Primer**
Tnf	CACCACGCTCTTCTGTCTAC	AGAAGATGATGATCTGAGTGTGAGG
Il1b	AACCTGCTGGTGTGTGACGTTC	CAGCACGAGGCTTTTTTGTTGT
Ccl20	AGAAGCAGCAAGCAACTACG	ACATCTTCTTGACTCTTAGGC
Ccl2	GCTCTCTCTTCCTCCACCAC	GCGTTAACTGCATCTGGCT
Ccl5	GCCCACGTCAAGGAGTATTT	TCGAGTGACAAACACGACTG
Cxcl2	ACCAACCACCAGGCTAGA	GCGTCACACTCAAGCTCT
Tgfb	ACGGAGAAGAACTGCTGTG	GGTTGTGTTGGTTGTAGAGG
FOS	CCTTCGGATTCTCCGTTTCTCT	TGGTGAAGACCGTGTCAGGA

Supplementary Methods:

Assessment of colitis: Experiments were performed using littermate mice cohoused for a week prior to the experiments. The disease activity index was estimated d as follows – 0 point were given for well-formed pellets, 1 for pasty and semi-formed stool, 2 for liquid stool, 3 for bloody smear along with stool, and 4 points were assigned for bloody fluid/mortality. Mice with more than 30% loss of bodyweight were considered moribund (51) , and euthanized. Data from moribund mice have not been included in the survival plot.

Colon length and histological studies: DSS-treated mice were euthanized, and the colon was excised. The colon length was measured as the length from the rectum to the caecum. Subsequently, distal colons were washed with PBS, fixed in 10% formalin and embedded in paraffin. 5μm thick sections were generated from the inflamed tissue and stained with hematoxylin and eosin (H&E). Alternately, sections were stained using H&E and Alcian Blue for revealing mucin content. Images were captured using Image-Pro6 software on an Olympus inverted microscope under a 20X objective. Epithelial damage and infiltration of inflammatory immune cells in the submucosa of the colon was assessed. For assessing intestinal permeability, FITC-dextran was gavaged to DSS-treated mice 6h prior to analysis of FITC fluorescence in serum.

Generation of bone marrow chimeras: Eight weeks old CD45.2+ or CD45.1+ mice were irradiated with 10 Gy of radiation and then administered retro-orbitally with 1-2 x107 bone marrow cells derived from tibia and femur of the donor CD45.1+ or CD45.2+ mice, respectively. After four weeks of transfer, chimerism was examined involving flow cytometric analyses of CD45.1 and CD45.2 markers on peripheral lymphocytes in the recipient mice. Subsequently, mice were treated with DSS.

Flow cytometric analyses: Flow cytometry was performed using FACS Verse flow cytometer (BD Biosciences). Data was analyzed using FlowJo v9.5 software (Treestar, Ashland and OR). Briefly, neutrophils were identified as Gr1+SiglecF- cells; macrophages and local dendritic cells as CD11b+F4/80+ and CD11c+F4/80-, respectively; and Th1, Th17 and Treg cells were recognized as CD4+IFNg+, CD4+IL17A+ and CD4+CD25+FoxP3+ cells, respectively.

qRT-PCR analysis: Total RNA was isolated using RNeasy Mini Kit (Qiagen, Germany) from IECs. qRT-PCR were performed using Power SYBR Green PCR master mix (Invitrogen) in ABI 7500 FAST instrument. Relative mRNA levels were determined using the $2^{-\Delta\Delta Ct}$ methods. Actin was used as a control.

Preparation of nuclear and cytoplasmic extracts from colon biopsies: Colon biopsies were homogenized and suspended in hypotonic cytoplasmic extraction buffer (10mM HEPES-KOH pH 7.9, 10mM KCl, 1.5mM $MgCl_2$, 1mM EDTA, 0.5% NP40, 5% sucrose, 0.75mM spermidine, 0.15mM spermine, 1mM DTT, 1mM PMSF). Samples were centrifuged at 8,000g, cytoplasmic extracts were isolated and nuclear pellets were resuspended in nuclear extraction buffer (250 mM Tris-HCl pH 7.5, 60mM KCl, 1 mM EDTA, 0.5 mM DTT, 1 mM PMSF). Nuclear pellets were subjected to three freeze-thaw cycles involving dry ice and 37^0C water bath, and nuclear extracts were isolated subsequent to centrifugation.